Available online at www.sciencedirect.com
SCIENCE DIRECT®
Journal of the European Ceramic Society 24 (2004) 3759–3767
www.elsevier.com/locate/jeurceramsoc

Writing conducting lines into alumina ceramics by a laser dispersing process

O. Baldus*, S. Schreck, M. Rohde

Forschungszentrum Karlsruhe GmbH, Institute for Materials Research I, P.O. Box 3640, 76021 Karlsruhe, Germany

Received 22 July 2003; received in revised form 5 December 2003; accepted 13 December 2003

Available online 6 May 2004

Abstract

The objective of this work is the development of a laser-supported process that allows to modify the electric and thermal properties of ceramics on a local scale. The principle of the process is based on local melting of the ceramic by a CO_2 laser beam and application of an additive to the molten area on the surface. During solidification, a metal–ceramic composite is formed with modified material properties compared to the bulk material. Different alumina samples were treated with metal powders of tungsten, copper, and oxides of these metals. Scanning electron microscopy (SEM) and energy-dispersive X-ray microanalysis (EDX) analysis reveal that the physical and chemical properties of a peripheral zone are changed in the heated region down to a depth of approximately 500 μm. The resulting resistance of the laser tracks can be adjusted from semi-conducting to metallic behavior with a resistivity down to 2×10^{-6} Ω/m. The modified ceramic can be used for heating elements working at operation temperatures of up to 1000 °C, high current resistance which can be loaded with current of up to 100 A.

Keywords: Composites; Al_2O_3; Electrical conductivity; Heating element; Laser treatment; Surface treatment; Conducting lines

1. Introduction

The demand for passive electric components of low resistance that carry high currents and dissipate electrical energy is increasing. For the packaging of integrated circuits and high integration, alumina ceramics are promising materials due to their low permittivity. To produce a thermally and electrically conducting structure on an alumina surface, brazing and thick-film deposition methods have been investigated for metallization.[1,7,14] An alternative way to produce, e.g., heating elements or resistors will be presented here.

The laser dispersing process allows for writing lines into a ceramic substrate and modifying the substrate properties. In contrast to metallic coatings, this process is faster and the substrate is modified on a local scale without lithographic process steps.

The laser-supported modification of alumina is based on laser heating and melting of the ceramic surface. During the absorption of the laser energy, the irradiated surface is heated in excess of the melting temperature and an additive (e.g., tungsten powder) is added to the melt pool. The high absorption of the CO_2 laser wavelength and the focus diameter determine the width of the melt pool which is typically 100–1000 μm. Rapid heating, melting, and solidification result in a high processing velocity. The mechanism of the laser dispersing process has already been described in a previous paper.[12,13] Marangoni convection and capillary force lead to the commingling of the additive and the molten substrate surface. In addition to marangoni convection which is controlled by temperature gradients, surface tension, and viscosity, the dispersing process is supported by the kinetic energy of the additive particles. When a critical fraction of the conducting phase in the composite produced is exceeded, an electrically conducting path is formed in accordance with percolation theory.[3] In the case of melting of the additive, the process is called laser alloying.[21] Here, wettability of the ceramic plays a significant role.[5]

A semi-conducting behavior has already been achieved by laser processing of alumina in a reducing environment.[16] Furnace and laser methods of bonding copper droplets to alumina ceramics have been investigated.[4] This study was carried out to investigate a process for producing conducting lines with nearly metallic properties in alumina. The ob-

* Corresponding author.
E-mail address: oliver.baldus@imf.fzk.de (O. Baldus).

0955-2219/$ – see front matter © 2004 Elsevier Ltd. All rights reserved.
doi:10.1016/j.jeurceramsoc.2003.12.008

jective of this work, however, was to improve the electrical properties by adjusting a well-defined ohmic resistance on the surface of the ceramic as well as to achieve good thermal coupling to the substrate by reducing crack formation.

2. Experimental

Two methods have been established for embedding secondary phases in a substrate material by a laser surface modification process. The *pre-coating process* can be divided into two steps. Firstly, the substrate is pre-coated with tungsten powder using a sedimentation method. The thickness of pre-coating varies between 30 and 200 μm. In the second step, the pre-coated and up to 1500 °C pre-heated substrate is exposed to laser irradiation. Pre-heating of the ceramic serves to reduce the risk of cracking induced by thermal shock. To prevent oxidation of the pre-coating, the whole process (pre-heating and laser process) takes place in a vacuum furnace equipped with a window that is transparent to laser light.[12] By means of the *powder injection process*, also referred to as one-step process, the additive is injected directly into the laser-induced melt pool via a nozzle of a conventional powder delivery system. A powder-feeding gas (here, argon) feeds the powder particles through a tube into the nozzle. The injection process allows for processing in air or under inert gas at ambient pressure. The samples are pre-heated to 1500 °C in a chamber and subsequently treated by the laser. Some experiments were performed without pre-heating of the ceramic sample. The injection process by the powder delivery system provides for additional degrees of freedom since the powder feed rate and the nozzle position can be adjusted. An exact positioning of the powder flow is important because the powder supply angle and the distance of the nozzle from the melting bath are critical parameters.

By both methods, the substrate is remolten locally by the laser beam and a composite of powder particles and the substrate material develops.[9] Fig. 1 illustrates these methods and shows the principle experimental setup. During the two-step process, no movement direction is preferred, whereas, the one-step process is preferably directed in accordance with powder particle flow.

For local melting, a CO_2 laser with a maximum power of 500 W was used (SM400, FEHA). Typical spot sizes of the focused laser beam varied between 0.2 and 1 mm. The applied laser power ranged from 5 to 400 W and the scanning velocity ranged from 10 to 10000 mm/min. Two different qualities of alumina substrates were used in the laser-supported modification process, i.e., alumina plates of 4 mm thickness (>99.7% Al_2O_3) and less than 5% open porosity, and dense alumina plates (96%) of 1 mm thickness. As additive, tungsten, copper, and copper oxide powder with particle sizes varying from approximately 1–100 μm were used.

Cross-sections of the microstructures of the manufactured lines were studied by light and scanning electron microscopy (SEM). Chemical compositions were analyzed qualitatively using an energy-dispersive X-ray microanalysis (EDX) system. The volume fraction of the phases was calculated using an image-analyzing software. The electrical resistance of the conducting paths obtained was determined by the four-point technique. Resistivity was calculated from the track width and length and the resistances measured. The current-carrying capacity was measured by soldering copper wires on the track. Simultaneously, the surface temperature of the sample was observed by a thermographic system.

3. Results

3.1. Two-step process

In Fig. 2, microscopies of cross-sections of laser-modified alumina ceramics (4 mm plates) are shown. Using optimized parameters by a repeated adjustment of the pre-coating thickness and laser power density, as shown in Fig. 2B, pore-free and crack-free composite material was produced. The solidification structure has the morphology reported for remelted laser tracks.[8,15] The bright particles in the melted zone consist of pure tungsten. A detailed analysis of the structure by SEM and EDX shows that the bright tungsten particles do not contain any oxygen. In contrast to the tungsten alumina oxide tracks which will be presented later in this paper, the composite in Fig. 2 contains no phases other than the substrate and the additive material. Hence, a metal–ceramic composite is produced. The corresponding result of the EDX analysis is shown in Fig. 3.

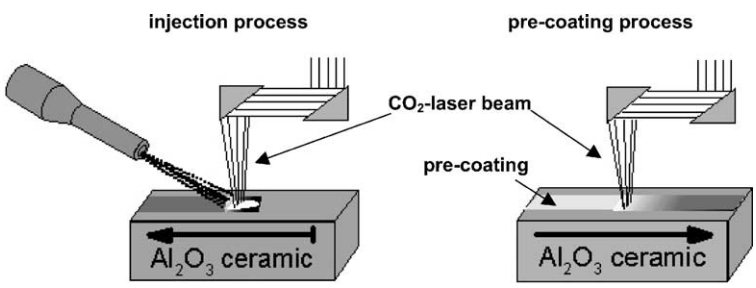

Fig. 1. Principle experimental setup.

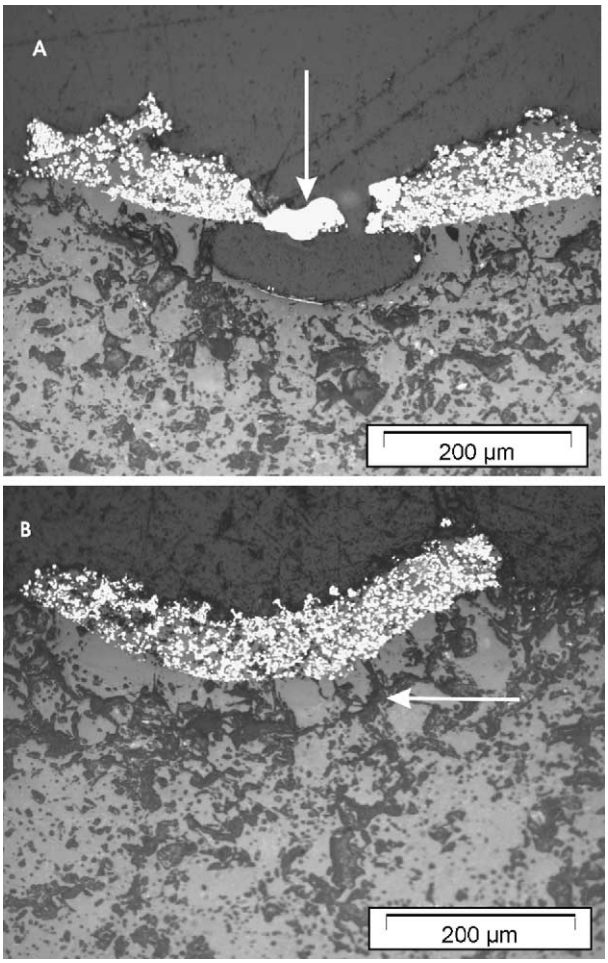

Fig. 2. Microscopy of the cross-section of laser tracks on pre-coated alumina substrates. Tungsten pre-coating thickness amounts to 100 µm. (A) Laser power 40 W at a rate of 1000 mm/min scan velocity; (B) 30 W at a rate of 1000 mm/min.

Molten tungsten particles appear as droplets with round edges, as obvious from Fig. 2A. The dispersed tungsten volume amounts to 40% (calculated from the black and white contrast in microscopy). Close to the narrow solidified melt pool, more cracks and pores are visible than in the substrate below (arrow in Fig. 2B). With increased power density, the metal particles in the center of the beam are molten (arrow in Fig. 2A). Due to the high temperature, a cavity develops in the center of the beam.[17] Temperature calculations confirm such high maximum temperatures (>3500 °C) in the melting pool.[6]

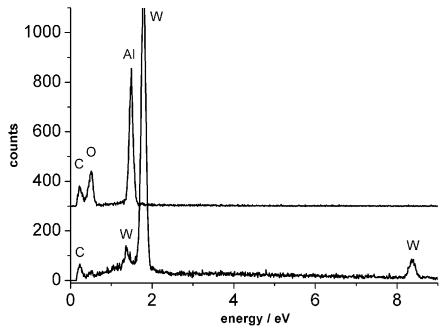

Fig. 3. EDX analysis of the sample in Fig. 2B. Lower curve, bright phase; upper curve, dark phase. The carbon peak results from the conducting coating that is needed for SEM.

The amount of dispersed powder in the track can be increased by a higher pre-coating thickness. Above 100 µm pre-coating thickness, however, the heat generated by the laser beam is not transferred sufficiently to the substrate. Hence, the melting depth decreases again, and consequently, so does the dispersed powder volume. This behavior can be explained by the lower temperature gradients at the surface which reduce the effect of the marangoni convection, and consequently, suppress the distribution of the metal particles within the reduced melt pool volume.[10] If the tungsten particle size amounts to approximately 1 µm and the adhesion of pre-coating is improved, maximum pre-coating thickness is limited only by the maximum power density which melts the substrate sufficiently and does not lead to thermally induced cracks in the substrate or sintering effects in the pre-coating. In addition, the maximum track width to be reached also limits the maximum applicable laser power density.[6] Best results were achieved with fine-grained tungsten powder (∼1 µm) which leads to a higher pre-coating density with less pores. Pores and cracks in the tungsten-enriched composite are also prevented by reducing the power density. This limits the dispersing depth to 100 µm as the number of cavities under the track rises drastically with increasing absorbed laser power (as shown in Fig. 2A).

The scanning velocity reached an optimum value at 1000 mm/min. Above this value, smaller dispersion rates were observed. Probably, a sintering effect at the surface of the coating blocked heat transfer and the mixing of the phases. Additionally, pores are more frequently observed at velocities lesser than 500 mm/min which is probably due to the inter-run undercut in traverse direction. This typical solidification structure at the surface of molten tracks[11] leads to regular pores below the composite at velocities lesser than 500 mm/min.

The resistance of the conducting lines can be as low as 2.7 Ω over a length of 50 mm. This corresponds to a resistivity of 3E−6 Ω m (bulk tungsten 0.05E−6 Ω m) and a surface resistance of 0.03 Ω.[1] When tracks longer than 10 mm are produced, interruptions may occur sometimes which lead to a decrease in the electrical conductivity. These interruptions are caused by pores that lead to a breakdown when applying a current higher than approximately 20 A for several seconds.

Using the two-step process, tracks can be produced with a low surface resistance and a high metal volume fraction in the ceramic matrix. A disadvantage of this two-step process results from the fact that the substrate is processed in an evacuated chamber and the poor absorption of laser light by

[1] Surface resistance [Ω] = resistance [Ω]* (track width/track length).

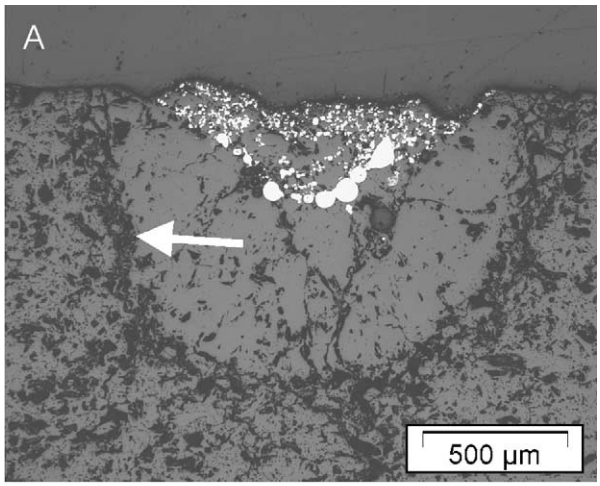

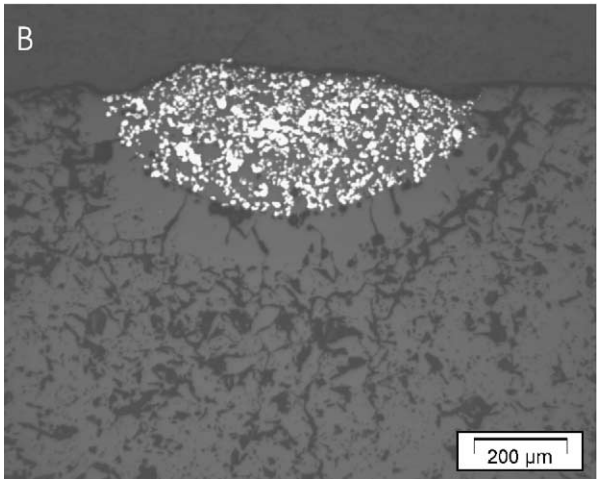

Fig. 4. Cross-section of laser tracks. (A) Laser power 80 W, scan velocity 75 mm/min, powder mass flow 0.4 g/min; (B) laser power 40 W, scan velocity 38 mm/min, powder mass flow 0.2 g/min.

strongly reflecting metals (e.g., copper). To overcome these disadvantages, the one-step process was studied.

3.2. The one-step dispersion process

In a first study, 4 mm thick alumina plates were modified with tungsten powder. The resulting microstructure is shown in Fig. 4. Melting depths are apparently higher than in the two-step process because higher laser power densities can be applied without a fracture of the sample. In Fig. 4A, the melting depth amounts to approximately 1 mm (100 μm in Fig. 2B). The penetration depth of the tungsten powder amounts to approximately 300 μm, such that the composite volume is increased. The molten and the dispersed areas are always well-defined. Up to the dispersion depth, the tungsten fraction in the composite amounts to 30% (Fig. 4A) or 40% (Fig. 4B). Electrical resistance of the tracks in Fig. 4A is 0.045 Ω. This results in 2E−6 Ω m or a surface resistance of 0.005 Ω (two-step: 3E−6 Ω m, 0.03 Ω). The capacity of these tracks to carry high electric currents will be outlined later in this paper. Cracks inside the tracks were not observed. In the surrounding substrate or at the interface between the track and the substrate, however, cracks occur (white arrow, Fig. 4A). Although the dispersion depth of tungsten can be increased with a higher laser power density, probability of thermal shock cracking increases as well. The different microstructure of the samples in Fig. 4 reveals this statement.

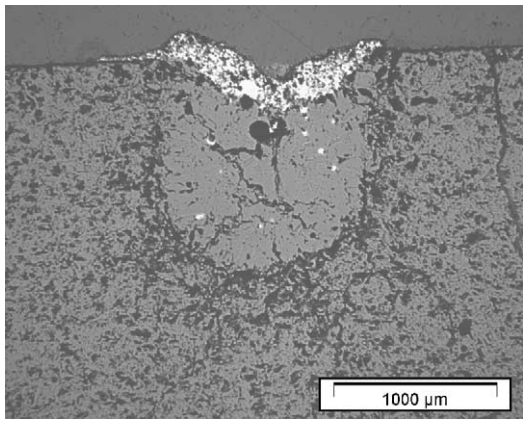

Fig. 5. Cross-section of a laser track. Laser power 80 W, scan velocity 75 mm/min, powder mass flow 0.4 g/min.

The parameters of powder feeding are very important to the one-step process. By moving the nozzle close to the melt pool and by increasing the injection angle to more than 70°, a high efficiency has been achieved with respect to the delivered and dispersed powder. An example of a low-dispersed powder volume is shown in Fig. 5. The injection angle was adjusted to 35° so that hardly any tungsten powder was dispersed into the melt pool.

The *powder feeding* rate has to be adjusted to meet certain requirements. At low rates, the dispersed volume is small. At high rates, the laser beam is blocked by the powder and the substrate will be coated. Application of a higher power density does not compensate the higher powder feeding rate. The track becomes unsteady with pores below the powder.

In relation to the dispersion depth and the development of pores, an optimum *powder particle size* exists. With small particles (1–5 μm APS), the maximum dispersion depth was lesser than 150 μm. This is shown in Fig. 6A. With big particles, more pores were observed, whereas, the dispersion depth was increased to more than 300 μm. Due to the higher kinetic energy of the coarse-grained metal particles, the penetration depth in the melt pool is increased and bubbles are generated. Use of powder with an average particle size of 12 μm produced the best results, as presented in Fig. 4A and B for example.

The *laser power density* controls the temperature in the melt pool and also the melt depth, melt width, and the thermal shock. Although powder injection partly removes heat from the molten substrate as does the powder-feeding gas, the laser power density mainly determines the maximum

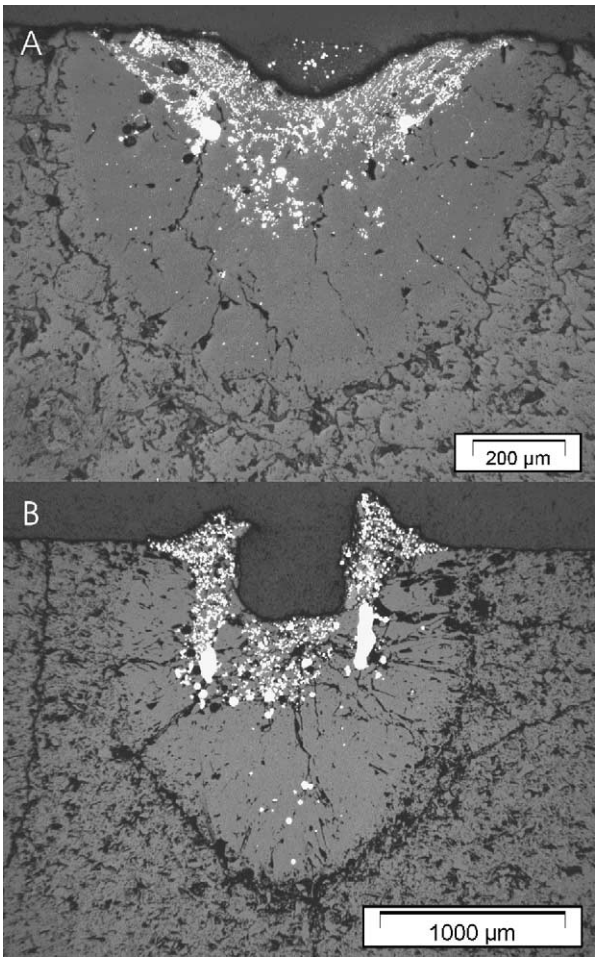

Fig. 6. Cross-section of laser tracks. (A) Laser power 60 W, scan velocity 75 mm/min, powder mass flow 0.3 g/min; (B) laser power 400 W, scan velocity 375 mm/min, powder mass flow 1.6 g/min.

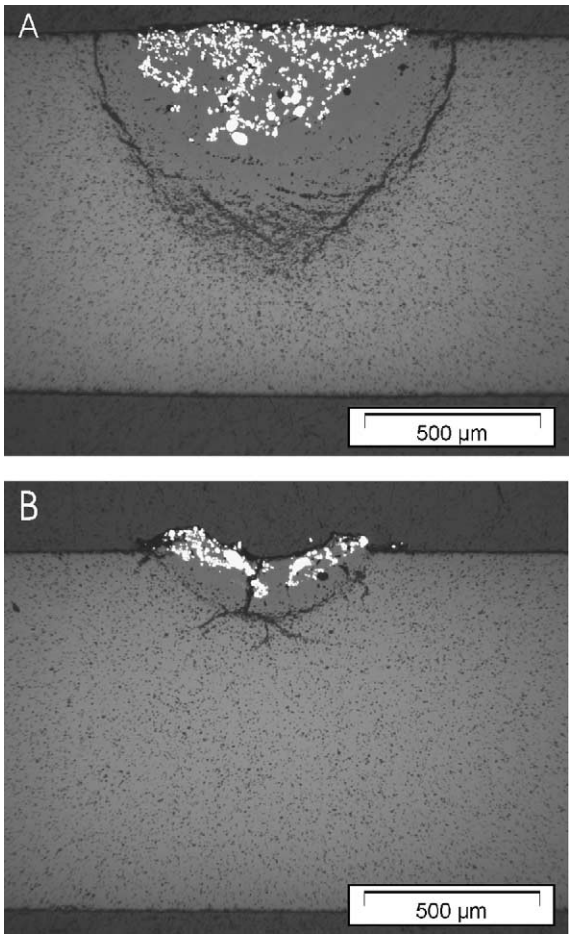

Fig. 7. Cross-section of laser tracks: (A) laser power 80 W at a rate of 300 mm/min, powder mass flow 0.4 g/min, pre-heating temperature 1500 °C; and (B) laser power 44 W at a rate of 150 mm/min, powder mass flow 0.15 g/min, room temperature.

temperature achieved. The laser power density must not lead to a keyhole-shaped surface or even a vapor capillary,[17] since the resulting tracks have less composite volume as a result of the material removed (Fig. 6B). Best results were achieved at lower velocities (<75 mm/min, Fig. 4B) compared to velocities higher than 75 mm/min (Fig. 4A). The undercut of the solidified melt causes interruptions in the trace if the laser power density is further increased.

The *atmosphere* plays a significant role for surface tension and its temperature coefficient that drives the marangoni convection. Since the one-step process could not be performed under vacuum, processing in air and under inert gas (argon) were compared. The melt pool was found to have slightly different shapes. Dispersion depth seemed to be approximately 10% higher under air. An advantage of processing with inert gas is the prevention of oxidation of the tungsten at the hot surface. This oxidation, however, does not change the structure of the tracks considerably in contrast to the laser alloying process which shall be outlined below. Due to the larger melt pool under air, processing in air was preferred. Literature data[5] show that oxygen decreases the surface tension of the molten ceramic. This effect is higher for the solid–liquid than for the liquid–vapor surface tension and, consequently, the contact angle between the metal and the liquid ceramic can be decreased drastically.[5] Such interactions are usually quantified by the activity coefficient of oxygen.

The *pre-heating temperature* was adjusted to 1500 °C (furnace temperature) or room temperature. The temperature of the substrate surface at the beginning of the laser process amounted to approximately 1200 °C. The impact of the substrate temperature on laser dispersing is now being discussed with thinner alumina substrates (1 mm) of reduced porosity. It is also intended to investigate the influence of the substrate thickness and structure on the laser process. In Fig. 7A, the less porous alumina substrate is treated at 80 W (at a rate of 300 mm/min) which leads to a melting depth of ~500 µm. This value nearly corresponds to that of the 4 mm substrates (Fig. 4). The high pre-heating temperature prevents the 1 mm substrate from cracking. If the laser power is increased or the pre-heating temperature decreased, the 1 mm substrate cracks, whereas, only small cracks are

generated inside the 4 mm substrates. Since pores can stop crack propagation,[21] the more porous material exhibits less damages by cracks than the dense alumina analyzed here. The laser power threshold for substrate cracking obviously is lower for these 1 mm substrates. Even at optimized parameters, some cracks between the track and the bulk material still occur. While producing a track longer than 50 mm, the sample cracked. This is a consequence of the cooling by heat emission of the thin alumina sample.

Thus, to produce demonstrators with a track length of 200 mm, samples were processed at *room temperature* at a power of 44 W (150 mm/min). This experiment (Fig. 7B) proves that conducting lines can be written into alumina at room temperature. The melt depth is measured to be 170 μm. Comparison of the melt pool widths of the tracks in Fig. 7 reveals the advantage of pre-heating for the dispersion process. At a higher substrate temperature, the melt pool volume and the dispersion depth can be increased. Additionally, the resistance of the pre-heated substrate to thermal shock increases. If the melt pool amounted more than half of the pre-heated substrate thickness, the substrate cracked during cooling down. Without pre-heating, the melt pool had to be below approximately a quarter of the sample thickness. Surface resistance of the sample in Fig. 7A is 0.6 Ω (1E−5 Ω m). The respective value of the sample shown in Fig. 7B is 0.4 Ω (1.8E−6 Ω m).

3.3. The one-step alloying process

Use of a modified one-step process resulted in a completely changed microstructure and composition. In Fig. 8A, SEM of a laser track cross-section is shown which was treated twice with the CO_2 laser beam under air. In a first run, a track was generated at a very high tungsten powder feeding rate. In the following run, this track was remolten by the laser beam. By this procedure, a completely different structure could be manufactured. During the second treatment with the laser beam, the tungsten powder was exposed to temperatures above 1000 °C so that complete oxidation occurred and a tungsten–alumina oxide compound developed. The tungsten–alumina oxide ($Al_xW_yO_z$)[19] which has a melting point of approximately 1200 °C wetted the alumina so well that the liquid phase filled all cavities in the laser-modified zone. A fine dendritic microstructure with tungsten oxide was produced in the ceramic with up to 57% of the matrix consisting of the metallic oxide (Fig. 8B). The interface between the molten zone and the substrate is free of cracks. This is an important improvement compared to the results of the dispersion experiments. Similar results have already been reported for hafnium oxide.[20] The dendrite structure is of semi-conducting character, which is probably due to the semi-conducting nature of tungsten oxide. EDX analysis revealed small additional phases of the system Al–W–O. The tungsten oxide phase was distributed in the entire substrate (arrow in Fig. 8A).

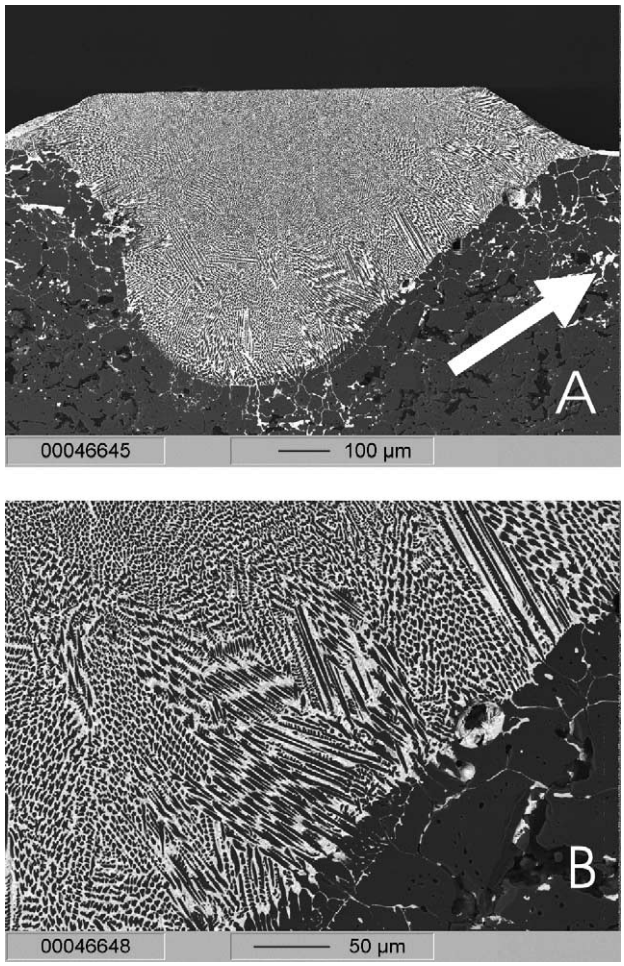

Fig. 8. SEM of the cross-section of laser-alloyed alumina with tungsten powder. (A) Laser power 68 W at 100 mm/min scan velocity and 1.5 g/min powder mass flow; and (B) laser power 53 W at 100 mm/min scan velocity.

As an alternative to tungsten powder, surface modification with copper was studied. The wettability of alumina at high temperatures by copper was investigated in many publications.[2,5] Without oxygen, no wetting between copper and alumina is possible. When using the same parameters as in the experiments with tungsten powder, only droplets of copper were produced with no continuous conductivity. When increasing the laser power, however, higher powder feeding rates and a pre-heating temperature of 1500 °C led to a continuous copper track on the ceramic surface (Fig. 9). Due to the low melting point of copper (1083 °C), the copper particles close to the laser melt pool were completely molten. Oxygen from the ambient air caused a partial oxidation of the copper and the temperature during the short heating time was sufficient for a copper–oxygen reaction. Thus, a copper oxide intermediate layer was formed (Fig. 9), which substantially improves wetting. Further EDX analysis confirmed copper–alumina–oxygen intermediate phases in the zone of fusion. Within the modified track, copper oxide precipitation was observed by EDX analysis. The electrical conductivity of the copper track was 5E−5 Ω m. However,

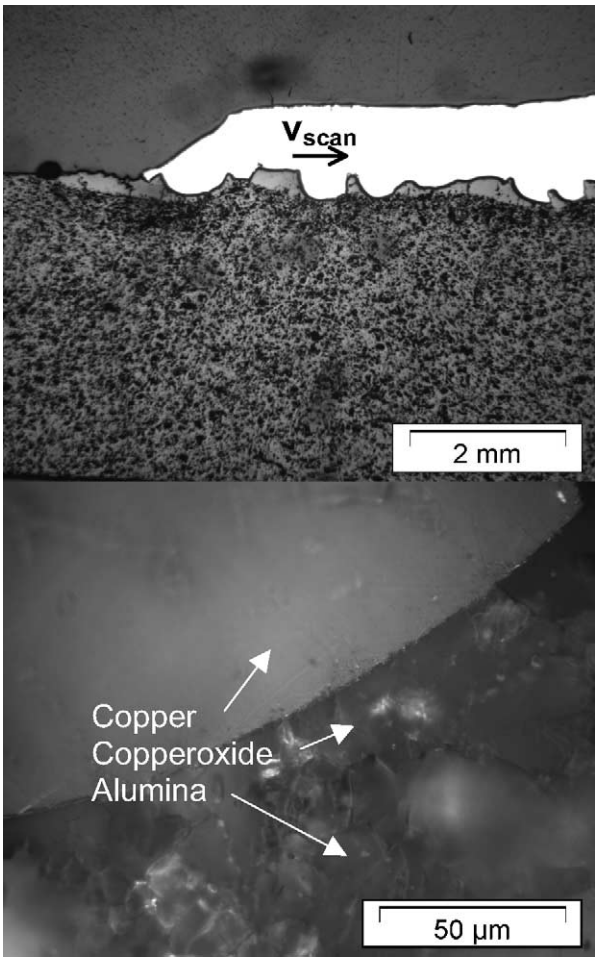

Fig. 9. Microscopy of a lengthwise section. Parameters: laser power 66 W, scan velocity 100 mm/min, powder mass flow 1.7 g/min, pre-heating temperature 1500 °C.

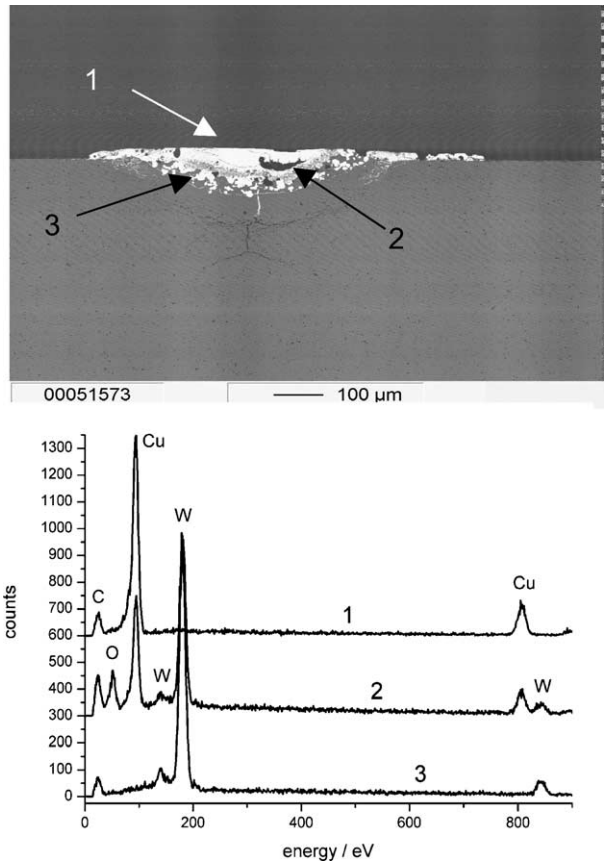

Fig. 10. Microscopy of the cross-section of W–CuO lines produced at room temperature. Laser power 34 W, scan velocity 100 mm/min, powder mass flow 0.5 g/min. Elements were identified by EDX analysis.

surface resistance was 0.3 mΩ which is lower than that of the tungsten track by an order of magnitude. The reason is that the large thickness of the copper track does not influence surface resistance. If the ceramic has ambient temperature at the beginning of the experiment, oxidation of the copper is not sufficient so that no wetting occurs.

Adding of pure copper(II) oxide to the melt pool led to remolten tracks with a Cu–Al–O dendrite phase (similar to Fig. 8). This new phase has excellent substrate wetting properties. The laser power density required was significantly lower than for tungsten tracks with a similar melting depth. Probably, the low melting temperature of the copper–alumina mixture (eutectic melting point ∼1150 °C)[2] leads to a low-melting phase during the laser process. The resistance of such alumina–copper oxide tracks ranges from 1 to 10 MΩ.

By mixing coper oxide with tungsten powder, copper was produced in addition to the dendrite phase in the laser-heated zone (Fig. 10). The tungsten powder was oxidized and the copper oxide reduced. This reaction takes place without pre-heating of the substrate such that a copper line is generated above the copper oxide–tungsten–alumina composite (Fig. 10). This is an important result with respect to the high thermal budget that is associated with the laser processing of alumina ceramics usually. By EDX analysis, several phases could be detected in the track (Fig. 10). In contrast to this, it was impossible to produce copper lines with copper powder at room temperature due to the bad wettability of the oxide ceramic. Thus, conducting lines could be manufactured at room temperature with a very low surface resistance of 0.005 Ω. Application of a current of 7 A to the track for 10 s did not damage the structure and led to a temperature of approximately 100 °C in the substrate.

Since resistivity is not the only important parameter under a high current load, the *current-carrying capacity* of the tracks was studied as well. This is illustrated in Fig. 7. Although the sample in Fig. 7B has the lower resistance, only the sample in Fig. 7A can be heated up to 400 °C by a current of 10 A without breakdown. At 5 A and 300 °C, a crack occurred in the sample of Fig. 7B. A current of 60 A was applied to the sample in Fig. 4B (also Fig. 13). After several seconds of track temperatures above 700 °C and cooling down, the resistance of the track was still the same. Consequently, a high-dispersed composite volume is more resistant to oxidation than a high-metal fraction near the sur-

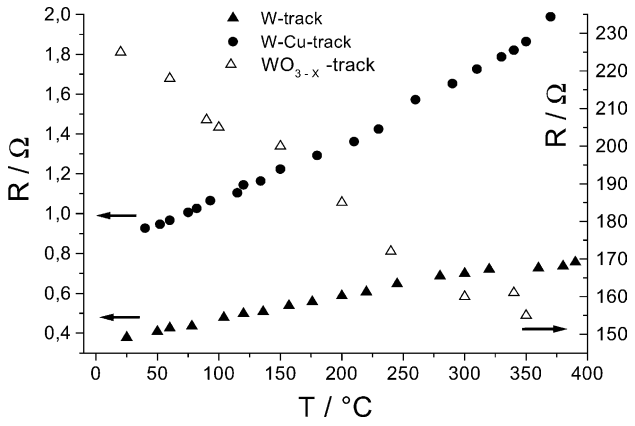

Fig. 11. Resistance as a function of temperature measured with a four-point technique. The temperature coefficient of the W and the W–Cu line is positive due to its metallic behavior, whereas, the WO_{3-x} line is negative which is typical of semiconductors.

face which leads to a very fast degradation of the resistance. When a current of 60 A is applied for more than 5 s, the track melts locally and tungsten oxide is formed resulting in a resistance of approximately 200 Ω (0.2 Ω before). Further heating for several seconds at constant current finally leads to a total degradation of the track at its most weak point. The dissipated power varies from 200 to 700 W for the tungsten tracks (e.g., Fig. 4) depending on the load duration. For the tungsten tracks produced at room temperature, it amounts to 80 W (Fig. 7B). The copper line shown in Fig. 9 was tested at a current of 100 A without any degradation being observed. The copper–tungsten track (Fig. 10) carried 7 A without any damage.

As a final result of these current-carrying experiments, it can be stated that the higher the dispersion depth is, the higher becomes the current-carrying capacity of the sample. Moreover, thermal coupling to the substrate determines the maximum duration of current application to the conducting track. Therefore, the solidification cracks at the interface between the resolidified material and the unmolten one has to be further reduced.

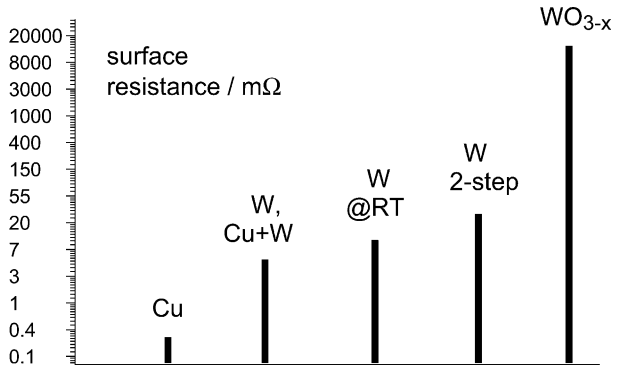

Fig. 12. Surface resistances of the conducting tracks produced.

The *resistance temperature coefficient* of the tungsten tracks amounts to 0.05 Ω/°C ± 0.02 (Fig. 11). This coefficient was measured between room temperature and 400 °C. It is in good agreement with the values of metallic conducting samples reported in literature.[18] The tungsten oxide track has a negative temperature coefficient which is characteristic of semi-conducting materials.

A survey of the surface resistances achieved is given in Fig. 12. The laser-induced copper tracks in the alumina substrate show the lowest resistances to be below 1 mΩ. The resistance of the tungsten tracks or the tungsten–copper tracks varies between 5 and 30 mΩ, whereas, the tungsten oxide exhibits a semi-conducting surface resistance of 20 Ω.

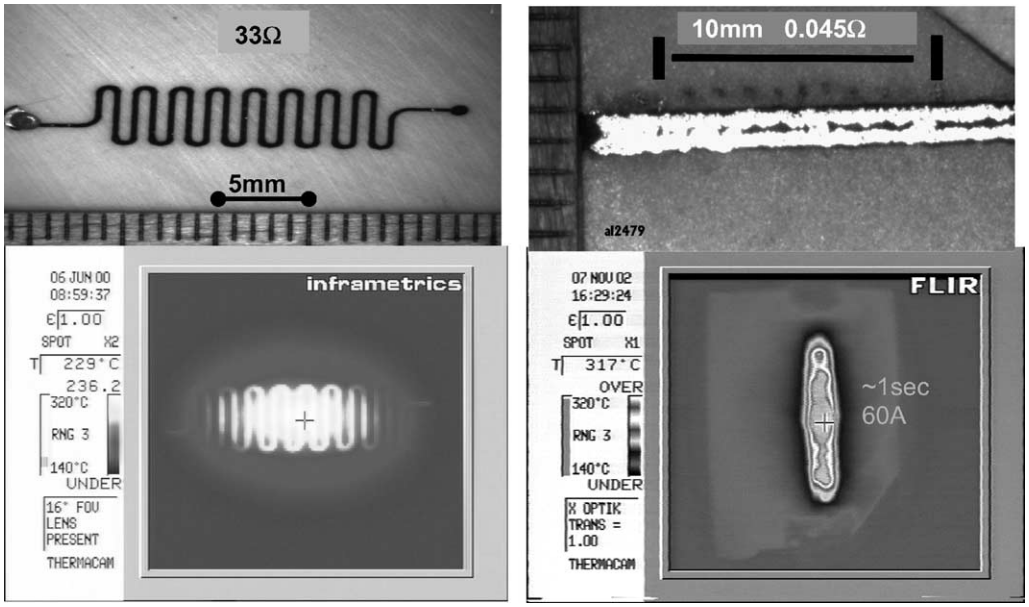

Fig. 13. Infrared camera picture of the heating element (left) and high-current resistor (right). Different temperatures correspond to different gray scales.

To test the applicability of laser-modified ceramic demonstrators, heating elements and resistors for high currents were manufactured. The demonstrators and screenshots of an infrared camera are presented in Fig. 13. The modified ceramics (top) are contacted with copper–titanium solder and then heated by direct current. The left sample is heated by 0.2 A up to approximately 229 °C. The right sample carries a current of 60 A for a few seconds. After a heating time of ∼1 s, a maximum temperature of 312 °C is reached.

4. Conclusions

The two-step process for laser dispersion of tungsten powder allows to produce conducting lines of very small resistivities down to one-sixtieth of the bulk resistance of the metal powder used. The process limits result from the homogeneity of pre-coating on one hand and the maximum melt depth of 100 μm on an average, on the other. Inhomogeneities of pre-coating generate pores or cavities, and the pre-coating itself prevents higher melting depths. This also limits the maximum current-carrying capacity that can be applied to the sample. The one-step process allows for higher dispersion depths and volumes and consequently, for an increased current-carrying capacity. With increasing melting depths and a larger volume of composite material formation, the thermal expansion mismatch leads to increased thermal stresses. By adjusting the parameters, this stress can be reduced such that even laser dispersion of non-pre-heated samples becomes possible. With such optimized parameters, a resistivity of $2E{-}6\,\Omega\,m$ and a surface resistance of $5\,m\Omega$ ($0.3\,m\Omega$ with copper) were achieved. If the desired resistance cannot be obtained, other additive materials (copper, tungsten oxide) could be employed. The laser alloying process with tungsten oxide and copper oxide results in a lamellar structure of the treated alumina surface. Since the melting point of the new metal-alumina composition is reduced towards pure alumina, melting with a reduced laser power density becomes possible. Resistance as a function of temperature of the tracks indicates a semi-conducting behavior. Application as high-power resistors or heating elements is possible due to the high currents carried by the tracks.

References

1. Akselesen, O. M., *J. Mater. Sci.* 1992, **27**, 1989.
2. Baldwin, M. D., Chidambaram, P. R. and Edwards, G. R., *Metall. Mater. Trans. A* 1994, **25A**, 2497.
3. De Bondt, S., Froyen, L. and Deruyttere, A., *J. Mater. Sci.* 1992, **27**, 1983.
4. Curicuta, V., Alexander, D. R. and Poulain, D. E., *Mater. Sci. Eng.* 2000, **B68**, 196.
5. Eustathopoulos, N., Nicholas, M. G. and Drevet, B., *Wettability at High Temperatures*, Pergamon Materials Series, Pergamon, 1999.
6. Gruhn, H., Heidinger, R., Rohde, M., Rüdiger, S., Schneider, J. and Zum Gahr, K. H., *Spring Meeting of the Materials Research Society*, San Francisco, CA, April 24–28, 2000.
7. Kapenieks, A., Eyett, M. and Bäuerle, D., *Appl. Phys. A* 1986, **41**, 331.
8. Lee, S. Z. and Zum Gahr, K. H., *Materialwissenschaft u. Werkstofftechnik* 1992, **23**, 117.
9. Mathias, E., U.S. Patent, No. 4496607, January 1985.
10. Mazumder, J., *Opt. Eng.* 1991, **30**(8), 1208.
11. Postacioglu, N., Kapadia, P. and Dowden, J., *J. Phys. D: Appl. Phys.* 1991, **24**(8), 1288.
12. Rüdiger, S., Gruhn, H., Heidinger, R., Rohde, M., Schneider, J. and Zum Gahr, K. H., *Surface Engineering, Euromat99, Vol 11*, ed. Dimigen, H. Wiley-VCH.
13. Schreck, S., Gruhn, H., Heidinger, R., Rohde, M., Schneider, J. and Zum Gahr, K. H., *Conference Proceedings, Materials Week*, September 2000.
14. Shafeev, G. A., *Appl. Phys.* 1992, **A55**, 387.
15. Shepeleva, L., Medres, B., Kaplan, W. D. *et al.*, *J. Laser Appl.* 1999, **11**(1), 38.
16. Stolz, B., *Dissertation*, Shaker Verlag, Aachen, 2000.
17. Tsukamoto, S., Kawaguchi, I. and Honda, H., *Sci. Technol. Weld. Joining* 2001, **6**(6), 363.
18. Van Vlack, L. H., *Materials Science for Engineers*, Addison-Wesley, 1970, p. 284.
19. Waring J. L., In *Phase Diagrams for Ceramists*, eds. Levin, E. M., Robbins, C. R. and McMurdie, H. F., American Ceramic Society, 1967, p. 97.
20. Zawrah, M. F., Schneider, J. and Zum Gahr, K. H., *Ind. Ceram.* 2002, **22**(2), 107.
21. Zum Gahr, K. H., Bogdanow, C. and Schneider, J., *Wear* 1995, **181–183**, 118.